PAPER *Special Section on Recent Progress in Measurement and Design Techniques on Antennas, Propagation and Wireless Systems*

The Numerical Analysis of an Antenna near a Dielectric Object Using the Higher-Order Characteristic Basis Function Method Combined with a Volume Integral Equation

Keisuke KONNO[†a)] *and* Qiang CHEN[†], *Members*

SUMMARY The higher-order characteristic basis function method (HO-CBFM) is clearly formulated. HO-CBFM provides results accurately even if a block division is arbitrary. The HO-CBFM combined with a volume integral equation (VIE) is used in the analysis of various antennas in the vicinity of a dielectric object. The results of the numerical analysis show that the HO-CBFM can reduce the CPU time while still achieving the desired accuracy.
key words: *Method of Moments (MoM), higher-order characteristic basis function method, volume integral equation*

1. Introduction

The Method of Moments (MoM) has been widely used for numerical analysis of integral equations [1], [2]. In recent years, fast MoMs such as the characteristic basis function method (CBFM), have been proposed for the analysis of large-scale problems [3]. In the CBFM, the original $N \times N$ matrix equation is reduced to a smaller $M^2 \times M^2$ matrix equation, and the reduced matrix is solved by the Gauss-Jordan method, where N is the number of segments and M is the number of blocks, respectively. It has been shown that the minimum CPU time of the CBFM is $O(N^{7/3})$ when the number of blocks $M \approx 0.9N^{1/3}$ [4]. In our research, the CBFM has been applied to the numerical analyses of small antennas in the vicinity of dielectric objects [5], [6]. The CPU time can be saved for the numerical analyses of small antennas in the vicinity of dielectric objects when $M = 0.9N^{1/3}$ and all antenna segments are allocated to the same block. However, decreasing CPU time can have a negative impact on accuracy. It is difficult to save the CPU time of the CBFM without allocating the antenna segments to different blocks when the size of the antenna in the vicinity of a dielectric object is more than several wavelengths. Moreover, it has been shown that the accuracy of the final results obtained using the CBFM becomes extremely poor when the antenna segments are allocated to different blocks [5], [6]. Therefore, the CBFM should be improved if it is used to analyze medium or large-sized antennas in the vicinity of dielectric objects.

Recently, the high order CBF, such as the tertiary basis function, has been proposed to enhance the accuracy of the CBFM and a connected patch array has been analyzed using the CBFM along with the tertiary basis function [7]. In this study, it has been demonstrated that the accuracy of the final results obtained using the CBFM can be enhanced by including the tertiary basis function and the fourth order CBF; however, the accuracy of the final results obtained by the CBFM with the high order CBF has not been proven successful for arbitrary block division because each block corresponds to a pair of patch elements. In addition, the numerical example was limited to the connected patch array antenna, and no numerical analysis results for other antennas have been found. On the other hand, a voltage source expression to enhance the quality of the primary CBF has been proposed and applied to the CBFM with the tertiary basis function [8]. Furthermore, it has been indicated that the higher-order CBFs beyond the tertiary basis have little impact on the accuracy of the final results; however, none of the numerical results obtained using CBFs beyond the tertiary basis were shown. In addition, the performance of the proposed CBFM has not been proven successful for arbitrary block division because the number of block divisions in the CBFM with the tertiary basis was limited to two. As described above, the higher-order CBFM has not been formulated in a general form. Moreover, the accuracy of the final results and the CPU time of the higher-order CBFM with arbitrary block division has not been quantitatively demonstrated.

In this paper, a higher-order CBFM (HO-CBFM) is clearly formulated in a general form. The HO-CBFM is capable of controlling both the accuracy of the final results and the CPU time without using singular value decomposition (SVD), which is used in the conventional third or fourth order of CBFM [7], [8]. Because the accuracy of the final results obtained by the HO-CBFM can be fully enhanced by the order of CBFs and the size of the overlapping region, the HO-CBFM allows for the arbitrary block division of antenna segments. As a result, the CPU time for the numerical analysis of medium or large-sized antennas in the vicinity of dielectric objects can be saved without the large compromise in accuracy. The performance of the HO-CBFM is clarified and compared with the conventional fourth order of CBFM.

This paper is organized into five sections. The principle and the formulation of the HO-CBFM is shown in Sect. 2.

The theoretical computational cost of the HO-CBFM is discussed in Sect. 3. In Sect. 4, the numerical analysis of various antennas in the vicinity of dielectric objects using the HO-CBFM is explained. Based on the results of the numerical analysis, both the accuracy of the final results and the computational cost of the HO-CBFM are shown. Section 5 is the conclusion.

2. The Principle and the Formulation of HO-CBFM

This section presents the formulation of the Lth order of the CBFM in a general form. Here, L represents the order of the HO-CBFM, and the conventional form of the CBFM corresponds to $L = 2$. A planar antenna, which is shown in Fig. 1, is chosen as an example to explain the algorithm of the Lth order of the CBFM. In the Lth order of the CBFM, the analysis model is divided into M blocks, which is also shown in Fig. 1, in which each block includes a number of segments. According to the block division of the analysis model, the Z matrix is divided into M^2 blocks, and both voltage/current vectors are divided into M blocks. In Fig. 2, N is the total number of segments, M is the number of blocks, K is the number of segments in a block, and K_o is the number of overlapping segments in an extended block. The extended block includes overlapping segments between adjacent blocks and is used to calculate the CBFs accurately. $\mathbf{Z}_{ik}^b$ represents $K \times K$ self/mutual impedance matrix between the ith block and kth block, and $\mathbf{V}_i^b$ and $\mathbf{I}_i^b$ represent the K-dimensional voltage and the current vector, respectively. Subscript b represents the block that does not include overlapping segments, while subscript e represents the extended block which includes overlapping segments.
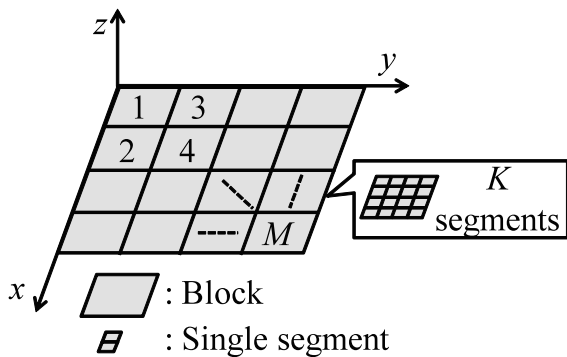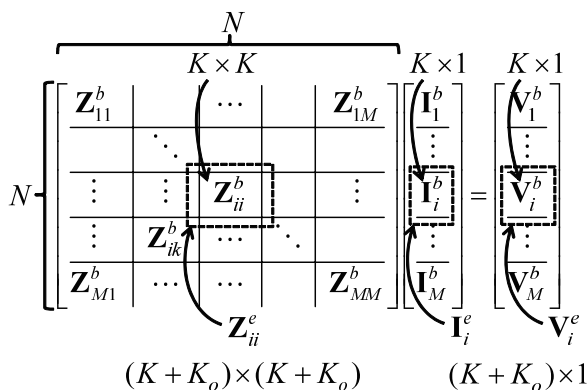
In the Lth order of the CBFM, an unknown block current can be expressed by following the equation,

$$\mathbf{I}_i^b = \alpha_{(i,i)}^{l=1}\mathbf{J}_{(i,i)}^{b(l=1)} + \sum_{l=2}^{L} \sum_{\substack{k=1 \\ i \neq k}}^{M} \alpha_{(i,k)}^{l}\mathbf{J}_{(i,k)}^{b(l)}, \tag{1}$$

$$(i = 1, 2, ..., M \quad \text{where} \quad L \geq 2),$$

where $\mathbf{J}_{(i,k)}^{b(l)}$ is the kth CBF of the lth order in the ith block and $\alpha_{(i,k)}^l$ is its weighting coefficient. The CBF is called the primary basis when $i = k$ and $l = 1$, while the CBF is called the secondary basis when $i \neq k$ and $l = 2$. The higher-order CBFs correspond to the CBFs of the $l \geq 3$ order.

The primary basis $\mathbf{J}_{(i,i)}^{b(l=1)}$ of the HO-CBFM can be obtained the same way as the conventional CBFM and is calculated from following $(K + K_o) \times (K + K_o)$ extended block matrix equation.

$$\mathbf{Z}_{ii}^e\mathbf{J}_{(i,i)}^{e(l=1)} = \mathbf{V}_i^e, \qquad (i = 1, 2, ..., M). \tag{2}$$

Equation (2) is solved using a direct solver, such as the Gauss-Jordan method, and the resultant inverse matrix $(\mathbf{Z}_{ii}^e)^{-1}$ is repeatedly used for calculating the higher-order CBFs. The primary basis $\mathbf{J}_{(i,i)}^{b(l=1)}$ is obtained by finding K components of $\mathbf{J}_{(i,i)}^{e(l=1)}$ and the remaining K_o components of $\mathbf{J}_{(i,i)}^{e(l=1)}$ corresponding to overlapping segments are discarded.

Next, the secondary basis $\mathbf{J}_{(i,k)}^{b(l=2)}$ is obtained from the following equations:

$$\mathbf{Z}_{ii}^e\mathbf{J}_{(i,k)}^{e(l=2)} = \mathbf{V}_{(i,k)}^e \text{ where } \mathbf{V}_{(i,k)}^e = -\mathbf{Z}_{ik}^{e'}\mathbf{J}_{(k,k)}^{b'(l=1)}, \tag{3}$$

$$(k = 1, 2, ..., i - 1, i + 1, ..., M),$$

where $\mathbf{Z}_{ik}^{e'}$ is a part of the block matrix $\mathbf{Z}_{ik}^e$ and its size is $(K + K_o) \times K'$. $\mathbf{J}_{(k,k)}^{b'(l=1)}$ is a part of the primary basis $\mathbf{J}_{(k,k)}^{b(l=1)}$ and its size is the K', where $K' = (K - K_o^{ik})$, and K_o^{ik} is the number of overlapping segments between the ith block and the kth block. The secondary basis $\mathbf{J}_{(i,k)}^{b(l=2)}$ is obtained by finding K components of $\mathbf{J}_{(i,k)}^{e(l=2)}$ and the remaining K_o components of $\mathbf{J}_{(i,k)}^{e(l=2)}$ corresponding to the overlapping segments are discarded.

The CBFs of the lth order are obtained from the sum of the CBFs of the $(l-1)$th order as follows:

$$\mathbf{Z}_{ii}^e\mathbf{J}_{(i,k)}^{e(l)} = \mathbf{V}_{(i,k)}^e \text{ where } \mathbf{V}_{(i,k)}^e = -\mathbf{Z}_{ik}^{e'}\sum_{\substack{k'=1 \\ k \neq k'}}^{M}\mathbf{J}_{(k,k')}^{b'(l-1)}, \tag{4}$$

$$(k = 1, 2, ..., i - 1, i + 1, ..., M, \quad l = 3, 4, ..., L),$$

the total number of CBFs is $M \times M_C$, where M_C is the number of CBFs in each block and $M_C = (L-1)(M-1) + 1$.

Fig. 1 Block division of planar antenna in HO-CBFM.

Fig. 2 Block division of matrix equation in HO-CBFM.

Because the CBFs obtained are not necessarily orthonormal, Gram-Schmidt orthonomalization is applied to the CBFs. After the orthonormalization, the original matrix equation is transformed into an expression using CBFs.

$$\sum_{i=1}^{M} \alpha_{(i,i)}^{l=1} \mathbf{u}_{(i,i)}^{l=1} + \sum_{l=2}^{L} \sum_{i=1}^{M} \sum_{\substack{k=1 \\ k \neq i}}^{M} \alpha_{(i,k)}^{l} \mathbf{u}_{(i,k)}^{l} = \mathbf{V}, \qquad (5)$$

$$(\mathbf{u}_{(i,k)}^{l} = [[\mathbf{Z}_{1i}^{b} \mathbf{J}_{(i,k)}^{b(l)}][\mathbf{Z}_{2i}^{b} \mathbf{J}_{(i,k)}^{b(l)}] \cdots [\mathbf{Z}_{Mi}^{b} \mathbf{J}_{(i,k)}^{b(l)}]]^{T}).$$

The inner product of two vectors are taken using Eq. (5) with $(\mathbf{u}_{(q,r)}^{l})^{*}$ when the Galerkin's method is applied. As a result, the original $N \times N$ matrix equation is transformed into an $(M \times M_C)^2$ reduced matrix, where $M \times M_C \ll N$. The weighting coefficient $\alpha_{(i,k)}^{l}$ is calculated using the reduced matrix equation using the Gauss-Jordan method. Finally, an unknown current vector is obtained after the CBFs and their weighting coefficients are substituted into Eq. (1).

Both the accuracy and the CPU time of the HO-CBFM depend on the total number of CBFs. Therefore, controlling the total number of CBFs is important in the HO-CBFM. In the CBFM shown in references [7] and [8], the higher-order CBFs corresponding to each of the lower CBFs are calculated. Because the number of the higher-order CBFs is the order of M^L, the total number of CBFs increases exponentially as a function of L. Therefore, singular value decomposition (SVD) is used to reduce the number of CBFs, and the total CPU time of the CBFM is controlled. On the other hand, the higher-order CBFs corresponding to the sum of the lower CBFs are calculated in the HO-CBFM as shown in Eq. (4). Because the total number of the higher-order CBFs is proportional to L, the total number of CBFs can be controlled linearly as a function of L. As a result, the CPU time and the accuracy of the HO-CBFM results can be easily controlled without using SVD.

3. The Computational Cost of the HO-CBFM

The computational cost of the HO-CBFM is shown in Table 1 and Table 2. Both the CPU time and the computer memory are functions of N, M, and L. The order L of the HO-CBFM slightly affects the computational cost unless L

Table 1 The order of the CPU time at each step of the HO-CBFM.

Matrix filling time	$O(N^2)$
Calculation of primary basis	$O(N^3/M^2)$
Calculation of CBFs ($l \geq 2$)	$O(LN^2)$
Gram-Schmidt orthonormalization	$O(M^2N)$
Calculation of $\mathbf{u}_{(i,k)}^{l}$	$O(LMN^2)$
Calculation of reduced matrix	$O(L^2M^4N)$
Inversion of reduced matrix	$O(L^3M^6)$

Table 2 The order of the computer memory for the HO-CBFM.

Impedance matrix	$O(N^2)$
HO-CBFs	$O(LM^2K)$
$\mathbf{u}_{(i,k)}^{l}$	$O(LM^2N)$
Reduced matrix	$O(L^2M^4)$

is more than or equals to N and M. Therefore, the order of the computational cost in the HO-CBFM is nearly independent of L when L is sufficiently small in comparison with N and M. As a result, it can be said that the minimum CPU time of the HO-CBFM is approximately $O(N^{7/3})$ when $M = 0.9N^{1/3}$ [4]. On the other hand, the computer memory cannot be saved using the HO-CBFM because the full impedance matrix must be obtained and stored in the computer memory; however, the computer memory of the HO-CBFM can be saved when the impedance matrix is stored on a hard disk. When the impedance matrix is stored on a hard disk and $M = 0.9N^{1/3}$, the computer memory of the HO-CBFM is $O(N^{5/3})$, but additional time for reading the impedance matrix is required.

4. Numerical Results

The HO-CBFM was applied for the numerical analysis of various antennas in the vicinity of uniform dielectric objects. In this analysis, an MoM based on the volume integral equation (VIE-MoM) was used because the VIE-MoM can be easily applied for the analysis of a non-uniform dielectric object. The volume integral equation was formulated using Richmond's MoM [2], [9]–[12].

The analysis models and their block division in the HO-CBFM are shown in Figs. 3 ~ 5. The analysis models shown in Figs. 3 and 4 consist of both an antenna and a uniform dielectric object. The antenna was divided into wire grid segments with the uniform radius a, while the dielectric object was divided into block dipole and monopole segments. The length of a wiregrid segment is $2\Delta l$. In the numerical analyses of these antennas, the arrangement of all segments was either parallel or perpendicular, and no segments were arranged diagonally. As a result, the multiple integral in the expression of self impedance and mutual impedance between block segments was reduced analytically using coordinate transformation [9]. Moreover, the symmetric property of the positions of block segments was used, and a significant amount of time was saved filling the impedance matrix. In addition to the antenna in the vicinity of the dielectric object, a helical antenna array with a finite ground plane that consists of both linear and curvilinear wire grid segments was analyzed as an example of typical antenna problems. The finite ground plane was constructed using wire grid segments, and several segments were placed diagonally near the feeding point of the helical antenna. N_x and N_y are the number of helical elements on the ground plane in the x and y direction, respectively. The delta gap source model was used as a feed model throughout these analyses. Antenna segments were allocated to different blocks to verify the enhancement of the accuracy of the HO-CBFM. The total number of segments and blocks in each numerical analysis model are shown in Table 3. The total number of blocks $M = M_x M_y M_z$ was set to approximately satisfy $M = 0.9N^{1/3}$. The extended block and the overlapping segments are defined by the size of the overlapping region w_e. Without including the overlapping region
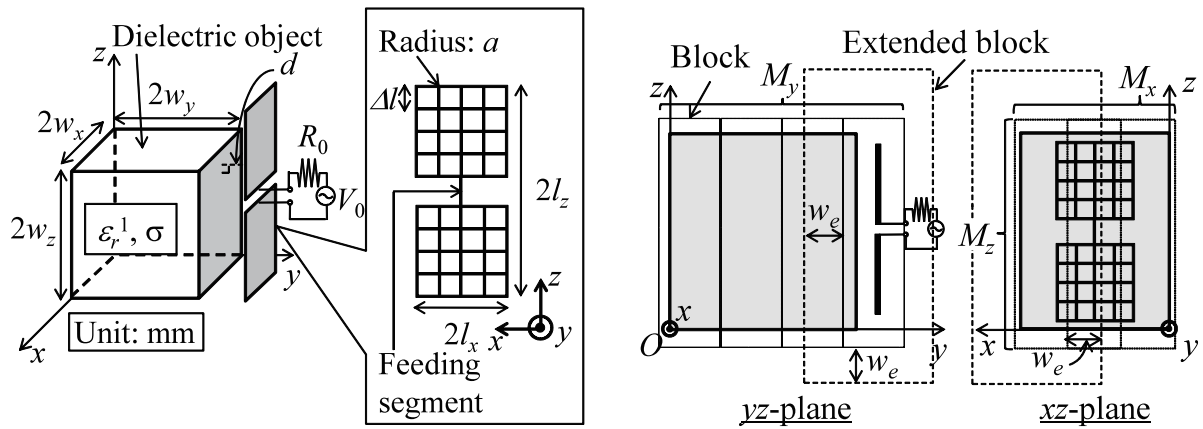
(a) A planar dipole antenna in the vicinity of a dielectric object.

(b) Block division.

Fig. 3   A planar dipole antenna in the vicinity of a dielectric object and its block division.
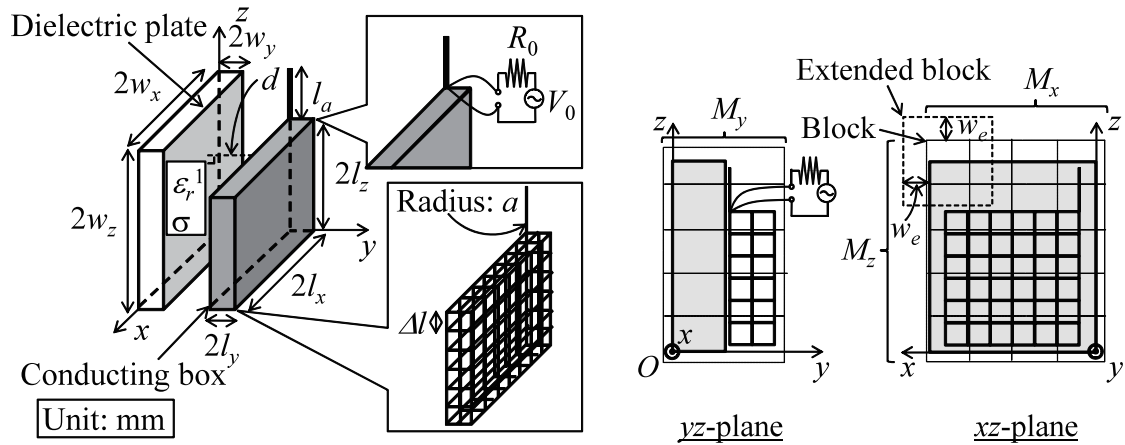
(a) A monopole antenna on the conducting box in the vicinity of a dielectric object.

(b) Block division.

Fig. 4   A monopole antenna on the conducting box in the vicinity of a dielectric object and its block division.
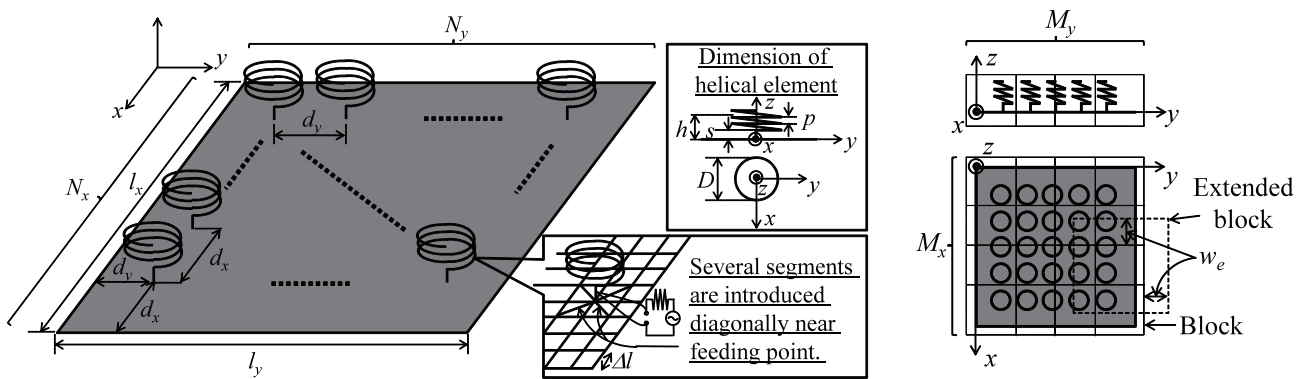
(a) A helical antenna array with a finite ground plane.

(b) Block division.

Fig. 5   A helical antenna array with a finite ground plane and its block division.

Table 3 Total number of segments and blocks in each analysis model.

Analysis model	Planar dipole antenna	Monopole antenna on conducting box	Helical antenna array with finite ground plane
Number of antenna segments N_A	469	2228	6875
Number of block dipole segments N_D	2649	3740	0
Number of block monopole segments N_M	642	1232	0
Total number of segments N	3760	7200	6875
Total number of blocks $M_x M_y M_z = M$	$1 \times 3 \times 5 = 15$	$5 \times 1 \times 4 = 20$	$4 \times 4 \times 1 = 16$
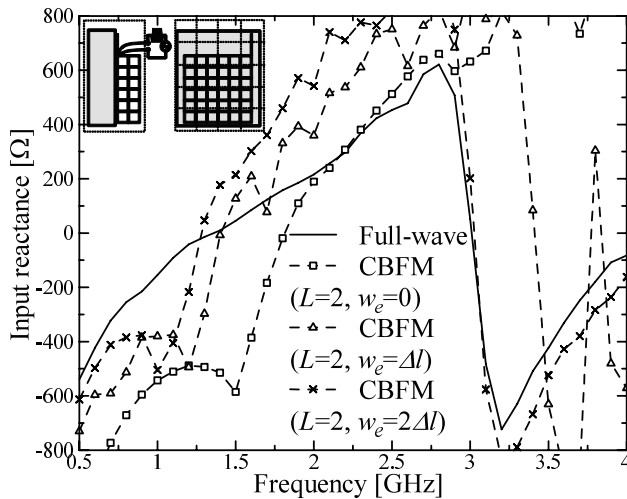
(a) The second order of the CBFM.
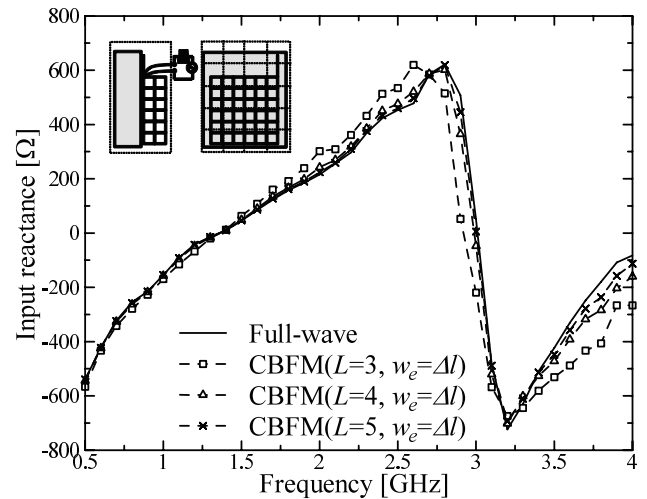
(b) The HO-CBFM.

Fig. 6 The input reactance of a monopole antenna on a conducting box in the vicinity of a dielectric object ($\epsilon_r^1 = 2$, $\sigma = 0$, $2w_x = 200$, $2w_y = 20$, $2w_z = 200$, $d = 2$, $2l_x = 200$, $2l_y = 20$, $2l_z = 150$, $l_a = 50$, $a = 0.1$, $\Delta l = 10$.).

(i.e. $w_e = 0$), the accuracy of the HO-CBFM is compromised because the CBFs obtained from the block matrices include fictitious edge effects. On the other hand, the quality of the CBFs is enhanced by including the overlapping region because the block matrices are extended and the fictitious edge effects are removed from the CBFs. As a result, the accuracy of the final results of the HO-CBFM is also improved. An Intel Core i7-3820 CPU with a 64 GB memory was used for numerical calculation.

The input reactance of the monopole antenna on the conducting box in the vicinity of the dielectric objects obtained by the second order of the CBFM and the HO-CBFM is shown in Fig. 6. The input reactance of the antenna cannot be obtained accurately using the second order of the CBFM even when the size of the overlapping region w_e is large. Because the number of CBFs in the second order of the CBFM is insufficient to obtain accurate results, it is difficult to improve the accuracy of the final results simply by increasing the size of overlapping region w_e; however, the input reactance of the antenna can be obtained accurately using the HO-CBFM because the number of CBFs are sufficient to obtain accurate results. Therefore, the accuracy of the final results obtained using the HO-CBFM are accurate even when the block division is arbitrary. The current density distribution of the monopole antenna on the conducting box is shown in Fig. 7. The accuracy of the current density distribution obtained using the CBFM becomes better as the order of the CBFM increases from $L = 2$ to $L = 3$. Because the HO-CBFs indicate multiple scattering between blocks, mutual coupling between the blocks can be calculated accurately using the HO-CBFs. As a result, the current and input reactance are obtained accurately using the HO-CBFM.

The relation between the CPU time and the accuracy of the proposed HO-CBFM is compared with the conventional HO-CBFM proposed in Ref. [7]. Singular value decomposition (SVD) was applied to the final set of CBFs obtained in the conventional HO-CBFM, and the remaining CBFs were used for calculating the reduced matrix. After applying the SVD, the CBFs with relative singular values above a certain threshold, ϵ were retained. The threshold ϵ was chosen by normalizing the singular values in comparison with the maximum values. The accuracy of the proposed and of the conventional HO-CBFM is quantitatively evaluated using following relative error,

$$\text{Relative error} = \frac{|\mathbf{I}_c - \mathbf{I}_f|}{|\mathbf{I}_f|}, \tag{6}$$

where $\mathbf{I}_f$ is the current obtained from the full-wave analysis and $\mathbf{I}_c$ is the current obtained from each CBFM.

Figures 8 ~ 10 show the total CPU time with the exception of the matrix filling time and the relative error of
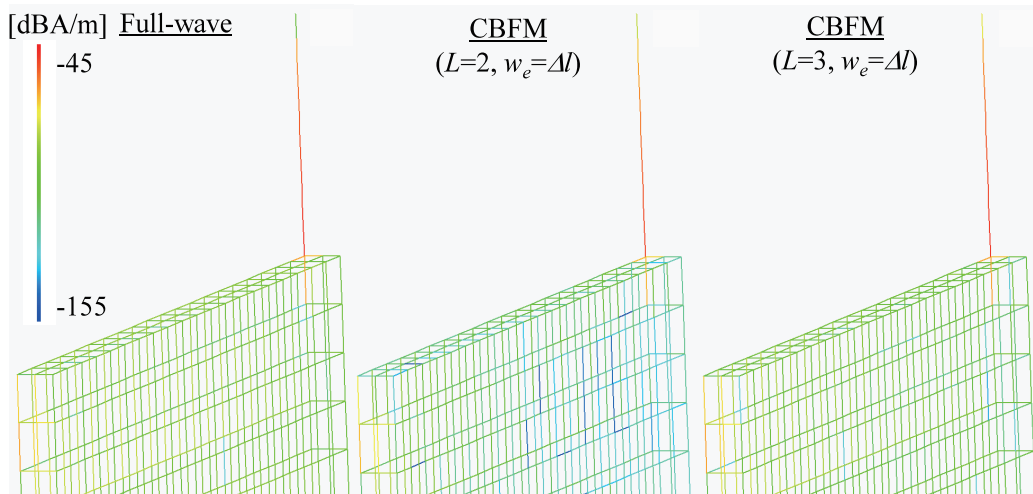
Fig. 7 The current density distribution of a monopole antenna on a conducting box in the vicinity of a dielectric object ($\epsilon_r^1 = 2$, $\sigma = 0$, $2w_x = 200$, $2w_y = 20$, $2w_z = 200$, $d = 2$, $2l_x = 200$, $2l_y = 20$, $2l_z = 150$, $l_a = 50$, $a = 0.1$, $\Delta l = 10$. The dielectric object is not shown in this figure.).
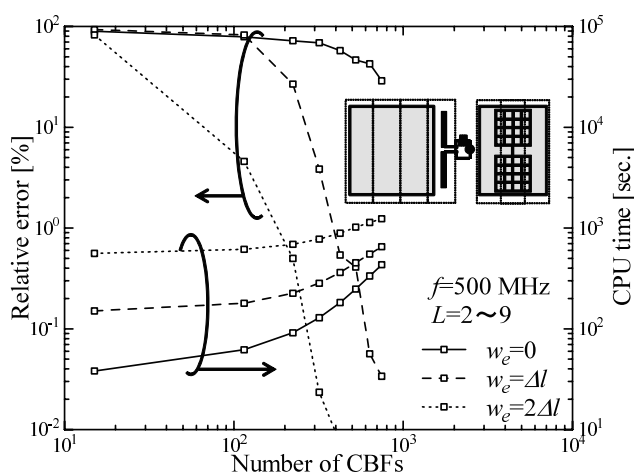
(a) The proposed HO-CBFM.
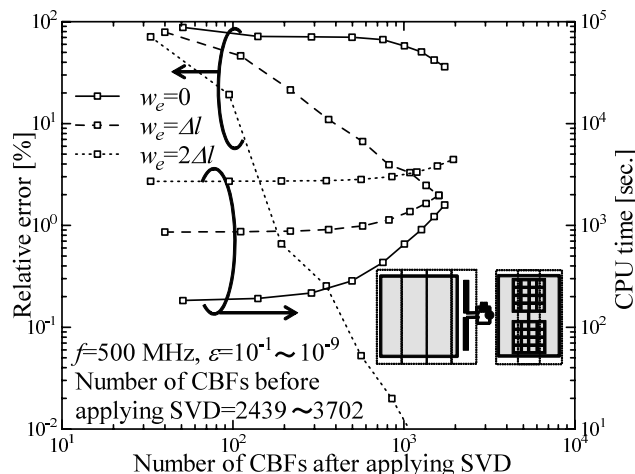
(b) The conventional fourth order of the CBFM.

Fig. 8 The CPU time and the relative error (A planar dipole antenna in the vicinity of a dielectric object. $\epsilon_r^1 = 2$, $\sigma = 0$, $2w_x = 30$, $2w_y = 130$, $2w_z = 90$, $d = 2$, $2l_x = 30$, $2l_z = 130$, $a = 0.1$, $\Delta l = 10$.).

the current obtained from the proposed and the conventional HO-CBFM. In Figs. 8(a) ~ 10(a), the number of CBFs increases as the order L increases. In addition, the number of CBFs after applying SVD increases as the threshold ϵ increases in Figs. 8(a) ~ 10(a). As shown in Figs. 8 ~ 10, the compromise between the accuracy and the CPU time is clearly seen in the results obtained using the proposed and the conventional HO-CBFM; however, in terms of the CPU time, the proposed HO-CBFM is more efficient than the conventional HO-CBFM. As explained in Sects. 2 and 3, the number of CBFs is proportional to L and linearly increases in the proposed HO-CBFM. Therefore, the number of CBFs need not be reduced via the SVD when L is sufficiently small. On the other hand, the number of total CBFs exponentially increases as a function of L in the conventional

HO-CBFM, and the excessive number of CBFs must be reduced via the SVD with threshold ϵ. Consequently, the CPU time of the conventional HO-CBFM is longer than the CPU time of the proposed HO-CBFM when the number of CBFs in the proposed HO-CBFM equals to the number of CBFs after applying SVD in the conventional HO-CBFM. Therefore, in terms of the CPU time, the proposed HO-CBFM is more efficient than the conventional HO-CBFM.

The relative error of the current obtained using the conventional and the proposed HO-CBFM heavily depends on the size of the overlapping region w_e. The size of the overlapping region w_e affects the quality of the CBFs. Because the CBFs are obtained using a block matrix equation that is truncated by fictitious edges, the CBFs include fictitious edge effects between adjacent blocks. In the conventional
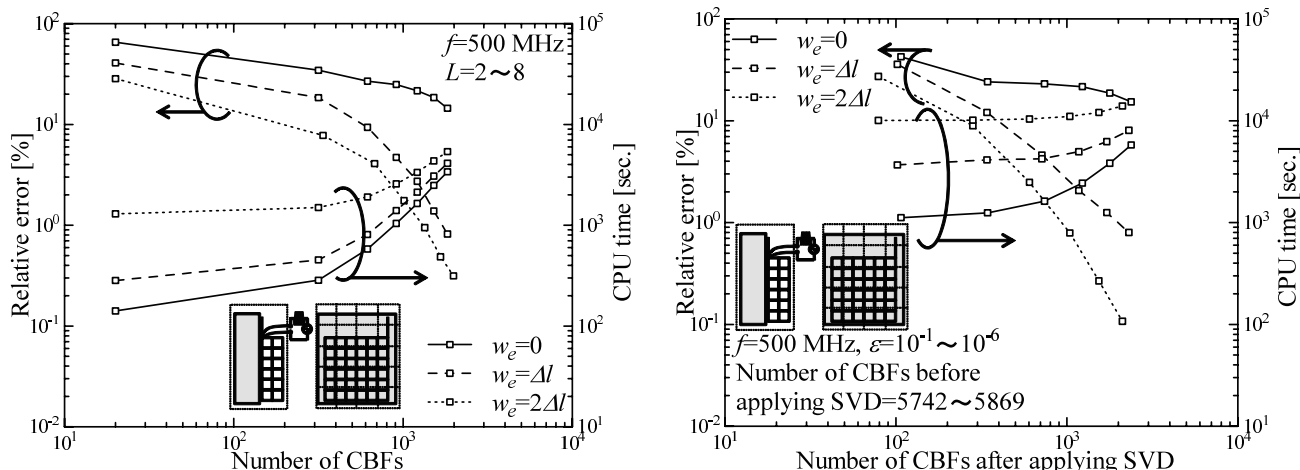
(a) The proposed HO-CBFM.

(b) The conventional fourth order of the CBFM.

Fig. 9   The CPU time and the relative error (A monopole antenna on a conducting box in the vicinity of a dielectric object. $\epsilon_r^1 = 2$, $\sigma = 0$, $2w_x = 200$, $2w_y = 20$, $2w_z = 200$, $d = 2$, $2l_x = 200$, $2l_y = 20$, $2l_z = 150$, $l_a = 50$, $a = 0.1$, $\Delta l = 10$.).
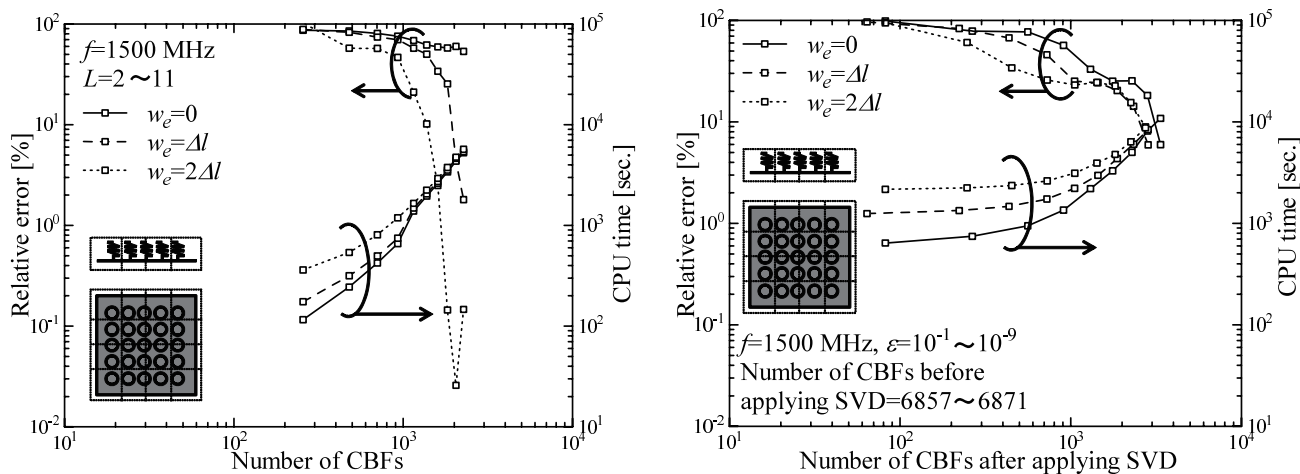
(a) The proposed HO-CBFM.

(b) The conventional fourth order of the CBFM.

Fig. 10   The CPU time and the relative error (A helical antenna array with a finite ground plane. $N_x = N_y = 5$, $h = 50$, $s = 10$, $p = 25$, $D = 50$, $l_x = 420$, $l_y = 420$, $d_x = 70$, $d_y = 70$, $\Delta l = 10$.).

and the proposed HO-CBFM, the current obtained by solving the original matrix equation before it is reduced is expressed approximately by the superposition of CBFs. Therefore, the CBFs must approximate the current distribution of the original problem as much as possible. Namely, the fictitious edge effects in the CBFs must be removed. The overlapping region between the blocks can alleviate the fictitious edge effects in the CBFs because the continuity of the current between the adjacent blocks is maintained by including the overlapping region. As a result, the relative error of the current obtained using the conventional and the proposed HO-CBFM with an overlapping region ($w_e = \Delta l$, $2\Delta l$) becomes much smaller than those without an overlapping region ($w_e = 0$).

In Fig. 10, the relative error of the current obtained using the proposed HO-CBFM shows a strong convergence in comparison with the conventional HO-CBFM. Because the helical antenna array with a finite ground plane has several feeding points, multiple scattering between blocks strongly affects the current in comparison with the other two models. In the conventional HO-CBFM, the HO-CBFs are orthonormalized and reduced by applying SVD with threshold ϵ, and the effect of multiple scattering in the current is partially lost. On the other hand, the HO-CBFs are orthonormalized using the Gram-Schmidt orthonormalization but not reduced in the proposed HO-CBFM. Thus, the current obtained using the HO-CBFM has an effect of multiple scattering.

In conclusion, the proposed HO-CBFM is effective for

the numerical analysis of various antennas even if its block division is arbitrary. Based on the results of the numerical analyses presented in this paper, the relative error is below 1% for the proposed HO-CBFM when the number of CBFs is from $\frac{N}{4}$ to $\frac{N}{3}$ and $w_e = 2\Delta l$. As shown in Fig. 10(a), the relative error of the current obtained using the proposed HO-CBFM may increase even when the number of CBFs increases. Similar results for the relative error of the current obtained using conventional HO-CBFM have been reported in previous studies [7]. The increase of the relative error is considered to be the results of numerical error.

5. Conclusions

In this paper, the HO-CBFM is clearly formulated and applied to the numerical analysis of various antennas in the vicinity of dielectric objects. Because the number of CBFs in the proposed HO-CBFM is proportional to L, the size of the reduced matrix in the HO-CBFM can be controlled easily using L. The results of the numerical analysis show that both the accuracy of the final results and the computational cost can be easily controlled in the proposed HO-CBFM even when the block division is arbitrary. The relationship between the performance of the HO-CBFM, the order L and the size of the overlapping region w_e was clarified.

Acknowledgments

References

[1] R.F. Harrington, Field Computation by Moment Methods, Macmillan, New York, 1968.

[2] J.H. Richmond and N.H. Geary, "Mutual impedance of nonplanar-skew sinusoidal dipoles," IEEE Trans. Antennas Propag., vol.AP-23, no.3, pp.412–414, May 1975.

[3] V.V.S. Prakash and R. Mittra, "Characteristic basis function method: A new technique for efficient solution of method of moments matrix equations," Microw. Opt. Technol. Lett., vol.36, no.2, pp.95–100, Jan. 2003.

[4] K. Konno, Q. Chen, K. Sawaya, and T. Sezai, "Optimization of block size for CBFM in MoM," IEEE Trans. Antennas Propag., vol.60, no.10, pp.4719–4724, Oct. 2012.

[5] K. Konno, Q. Chen, K. Sawaya, and T. Sezai, "Analysis of linear antenna near dielectric object by CBFM," Proc. IEEE AP-S Int. Symp., 263, pp.1–2, July 2012.

[6] K. Konno, Q. Chen, and K. Sawaya, "Optimum block division in CBFM for fast MoM," Proc. IEICE Int. Symp. Antennas. Propag., 3D1-1, pp.910–913, Oct.-Nov. 2012.

[7] S.G. Hay, J.D. O'Sullivan, and R. Mittra, "Connected patch array analysis using the characteristic basis function method," IEEE Trans. Antennas Propag., vol.59, no.6, pp.1828–1837, June 2011.

[8] G. Bianconi, C. Pelletti, and R. Mittra, "A high-order characteristic basis function algorithm for an efficient analysis of printed microwave circuits and antennas etched on layerd media," IEEE Antennas Wireless Propag. Lett., vol.12, pp.543–546, 2013.

[9] D. Koizumi, Q. Chen, and K. Sawaya, "Galerkin-MoM analysis for dielectric scatters by using sinusoidal reaction technique," Proc. IEEE AP-S Int. Symp., vol.2, pp.526–529, July 2001.

[10] H. Zhai, Q. Yuan, Q. Chen, and K. Sawaya, "Single integral expressions of self/mutual impedance of volume sinusoidal monopoles with consideration of endpoint charges," IEICE Technical Report, AP2007-156, Jan. 2008.

[11] M.A. Tilston and K.G. Balmain, "On the suppression of asymmetric artifacts arising in an imprementation of the thin-wire method of moments," IEEE Trans. Antennas Propag., vol.38, no.2, pp.281–285, Feb. 1990.

[12] A. Köksal and J.F. Kauffman, "Mutual impedance of parallel and perpendicular coplanar surface monopoles," IEEE Trans. Antennas Propag., vol.39, no.8, pp.1251–1256, Aug. 1991.

Keisuke Konno received the B.E., M.E., and D.E. degrees from Tohoku University, Sendai, Japan, in 2007, 2009, and 2012, respectively. Currently, he is an Assistant Professor in the Department of Communications Engineering at the Tohoku University. His research interests include computational electromagnetics and array antennas. He is a member of IEEE and IEICE. He received the Encouragement Award for Young Researcher and Most Frequent Presentations Award in 2010 from the Technical Committee on Antennas and Propagation of Japan, Young Researchers Award in 2011 from the Institute of Electronics, Information and Communication Engineers (IEICE) of Japan, IEEE EMC Society Sendai Chapter Student Brush-up Session & EMC Sendai Seminar Student Best Presentation Award in 2011.

Qiang Chen received the B.E. degree from Xidian University, Xi'an, China, in 1986, the M.E. and D.E. degrees from Tohoku University, Sendai, Japan, in 1991 and 1994, respectively. He is currently a Professor with the Department of Communications Engineering, Faculty of Engineering, Tohoku University. His primary research interests include antennas, microwave and millimeter wave, electromagnetic measurement and computational electromagnetics. Dr. Chen received the Young Scientists Award in 1993, the Best Paper Award and Zen-ichi Kiyasu Award in 2009 from the Institute of Electronics, Information and Communication Engineers (IEICE) of Japan. Dr. Chen is a senior member of the IEEE and member of the IEICE. He was the Secretary and Treasurer of IEEE Antennas and Propagation Society Tokyo Chapter in 1998, the Secretary of Technical Committee on Electromagnetic Compatibility of IEICE from 2004 to 2006, the Secretary of Technical Committee on Antennas and Propagation of IEICE from 2008 to 2010, Associate Editor of IEICE Transactions on Communications from 2007 to 2012. He serves as Chair of IEICE Technical Committee on Photonics-applied Electromagnetic Measurement, Vice Chair of IEEE Antennas and Propagation Society Japan Chapter.